

Donor deactivation at high doping limit: donor pair and impurity band model

Chihak Ahn and Woosung Choi
Device Lab

Samsung Semiconductor Inc.
3655 North 1st street, San Jose, CA 95134
Email: chihak.ahn@samsung.com

Hiroyuki Kubotera and Yasuyuki Kayama
Samsung R&D Institute Japan
2-7, Sugawachō, Tsurumi-Ku
Yokohama, Kanagawa 230-0027, Japan

Alexander Schmidt, Keunho Lee, Youngkwon Park
Semiconductor R&D Center,
Samsung Electronics Co., Ltd.
San16 Banwol-Dong, Hwasung-Si,
Gyeonggi-Do, South Korea, 445-701

Nick.E.B Cowern
School of Electrical and Electronic Engineering,
Merz Court, Newcastle University
Newcastle upon Tyne, UK NE1 7RU

Abstract—We present a donor deactivation model at high doping limit. The limitation of the existing activation model is discussed and a solution is proposed. In the new model, the impurity band model is combined with *ab-initio* based lattice Monte Carlo (LMC) simulation to explain the saturation behavior of active donor concentration experimentally observed. The developed impurity band model can reproduce the activation level correctly and improves our understanding of charge carrier distribution in the impurity band. It also provides a new aspect of the behavior of the Fermi level (E_F) at high doping limit. As a result, incorporating the new models into the existing diffusion and activation model improves the predictability of donor activation level.

I. INTRODUCTION

At moderate donor doping condition ($< 5 \times 10^{20} \text{cm}^{-3}$), donor activation can be described reasonably well with a simple transient dopant activation model in which clustered dopants and isolated substitutional dopants co-exist and each can transform into the other by clustering or dissociation while the unclustered dopants are diffusing. In the model there is an important assumption that all un-clustered substitutional dopants are active. The assumption is the basis of dopant activation model in the commercial process simulator [1] and it leads to a very high active donor concentration ($\sim 8 \times 10^{20} \text{cm}^{-3}$) when extremely highly doped sample is annealed at high temperature for a short time. Fig.1 shows the overestimated activation level when the existing model is used. To understand the physical deactivation mechanism and correct for the overestimated activation, an impurity band model and dopant pair model are suggested.

II. DONOR PAIR MODEL

Previously Müller showed that closely spaced donor pairs produce deep energy levels in the bandgap using *ab-initio* calculations and a significant fraction of substitutional donors becomes inactive at high doping concentration using analytic statistical methods [3]. Also it is shown that donor pairs are fully inactive at the first nearest neighbor configuration and unstable δ^3 defects generated by donor pairs up to the eighth nearest neighbor spacing are considered to describe the observed large fraction of inactive substitutional donors in low temperature molecular beam epitaxy samples. In our model, only the local energy minimum structure of pairs is considered and the saturation

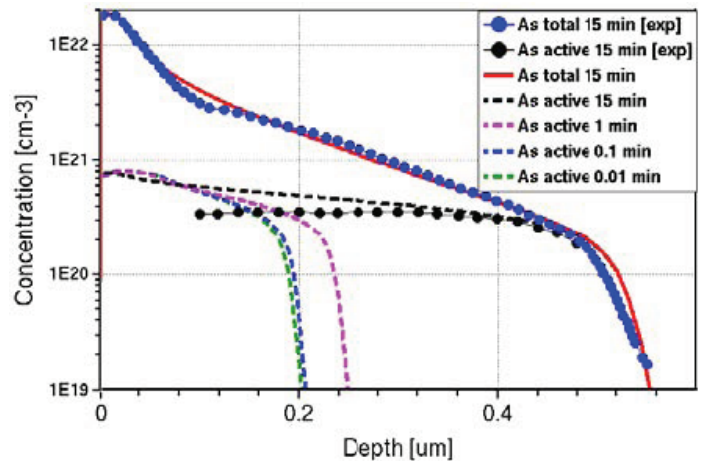


Fig. 1: The time evolution of simulated As active concentration and comparison between simulation and measurement [2] for 15 min annealing at 1050°C with $1.5 \times 10^{17} \text{cm}^{-2}$ dose implant.

behavior of the active concentration can be explained without the unstable δ^3 defects. As a result, our model gives a growing activation with increasing temperature when no cluster exists, which is opposite to Müller's δ^3 defect model (compare Fig.4.9 in Ref.[3] and Fig.6). Using density functional theory (DFT) software, Vienna *ab-initio* simulation package (VASP) [4], we investigated the energy level of a donor in the proximity of other donor or donor-defect cluster at various distances and the result is shown in Fig 2. For donor pairs and donor-donorcluster pairs, the 1st nearest neighbor (1NN) pair has a much deeper energy level than other pairs. In our model, 1NN donor pairs are assumed to be fully inactive which is the same as in Ref. [3] and partial activation is allowed for 1NN donor-donorcluster pairs. At longer distance (2NN and 3NN), it is clearly shown that donor pairs still make lower energy states than the maximally spaced donors (2.8 nm case in Fig. 2). However, quantitative modeling of inactive donor fraction using the *ab-initio* DOS has a limitation because the band structure itself is not accurate enough for this purpose. Therefore, pairs at 2NN or beyond are treated as the conventional band broadening in the impurity band model and we apply the lattice Monte Carlo (LMC) model to count only 1NN donor-

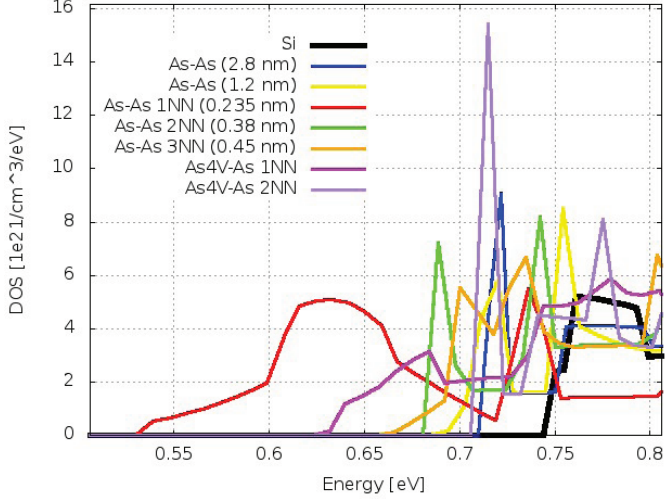


Fig. 2: Density of states near the conduction band minimum for various arsenic configurations calculated by density function theory. Calculation was done using 216-atom supercell with 4^3 \vec{k} -points. In all cases, the valence band maximum is set to the reference energy.

donor pair and donor-donor cluster pairs.

III. IMPURITY BAND MODEL

In the conventional process models, room temperature activation and high temperature activation are identical. However, they can be considerably different at extreme doping condition considered in this study. Therefore, experimentally measured activation level at room temperature needs to be differentiated from the high temperature activation used in diffusion simulation, which can be explained by the impurity band model.

At low doping condition, dopants are well separated and thus there is no overlap between wave functions of bound charge carriers. As a result, dopants generate highly degenerated single dopant energy level. As the isolated substitutional donor concentration increases, the wave functions start overlapping each other, which lifts off the degeneracy and turns the discrete impurity level into the impurity band. Eventually the broadened impurity band touches the conduction band edge to make the band structure metallic. This phenomenon is known as metal-insulator transition [5]. For phosphorus (P), the metal-insulator transition occurs when doping concentration is $3.7 \times 10^{18} \text{ cm}^{-3}$ [6]. Above the concentration, the chemical potential of electrons is closer to the CBM of undoped Si and the integrated impurity band DOS becomes comparable to the effective density of states. Therefore, we need to consider the shape of the total DOS including impurity band and the tailed conduction band. Based on the previous report [7], the Gaussian shape impurity band model is used in our study.

$$\rho_i(E) = \frac{2N_D}{\Delta E_D} \exp\left(-4\pi \left(\frac{E - E_D - \Delta E_i}{\Delta E_D}\right)^2\right), \quad (1)$$

where N_D is the dopant concentration excluding clustered dopants, ΔE_D is the impurity band width, E_D is the impurity energy level at low concentration limit, ΔE_i is the shift of the center of the impurity band. In Ref. [7], ΔE_D was calculated with hydrogen atom model using the conduction band DOS effective mass for the bound electron at donor site, which is controversial. Instead of using the model, here we simply use

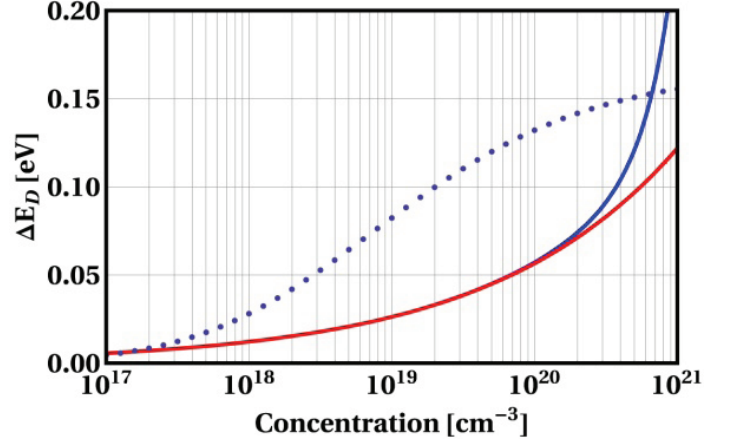


Fig. 3: ΔE_D as a function of dopant concentration. Dotted line is the model in Ref [7] and the blue solid line is our model with the concentration dependent α factor. The red solid line is with $\alpha = 1$

the Coulomb interaction energy to estimate the bandwidth. The magnitude of the Coulomb interaction between the two charges is given by

$$\Delta E_D \approx \alpha(N_D) \frac{q^2}{4\pi\epsilon(N_D)^{-1/3}}, \quad (2)$$

where ϵ is the dielectric constant of Si, $(N_D)^{-1/3}$ is the average distance between the closest donors and $\alpha(N_D)$ is a scaling factor of order 1. Fig. 3 shows the difference between the Ref. [7] and our simple model with $\alpha = 1 + (N_D/N_{ref})^2$ where $N_{ref} = 10^{21} \text{ cm}^{-3}$. Although $\alpha(N_D)$ is introduced mainly as a calibration factor, it also has a physical meaning which is discussed in the next section.

For ΔE_i , the same model equation as Ref. [7] is used with the Bohr radius directly calculated from the donor energy level.

$$\Delta E_i = \frac{q^2\xi}{4\pi\epsilon} \left(\frac{3}{8} - \frac{2\xi\lambda_e \sin\left(\frac{1}{2\xi\lambda_e} + 2 \tan^{-1}\left(\frac{1}{8\xi\lambda_e}\right)\right)}{4 + 1/(16\xi^2\lambda_e^2)} \right), \quad (3)$$

$$\xi = \frac{1}{a_B} = -\frac{4\pi\epsilon E_D}{q^2}, \quad (4)$$

$$\lambda_e = \sqrt{\frac{\epsilon kT}{q^2 n}}, \quad (5)$$

where λ_e is the screening length, k is the Boltzmann constant, T is the absolute temperature and n is the total electron concentration. Finally, conduction band tailing is calculated as described in Ref. [7]. In the model, the parabolic conduction band is perturbed by randomly distributed donor potential.

$$\rho_c(E) = \int_{-\infty}^E \frac{6\sqrt{2}(m^*)^{3/2}}{\pi^2\hbar^3} \sqrt{E - V} p(V) dV, \quad (6)$$

$$p(V) = \frac{1}{\sqrt{2\pi}\sigma} \exp\left(-\frac{V^2}{2\sigma^2}\right), \quad (7)$$

$$\sigma = \sqrt{\frac{N_D + N_A}{8\pi^2\epsilon^2}} q^4 \lambda \quad (8)$$

where \hbar is the reduced Planck's constant, m^* is the effective electron DOS mass, N_A is the acceptor concentration, and λ

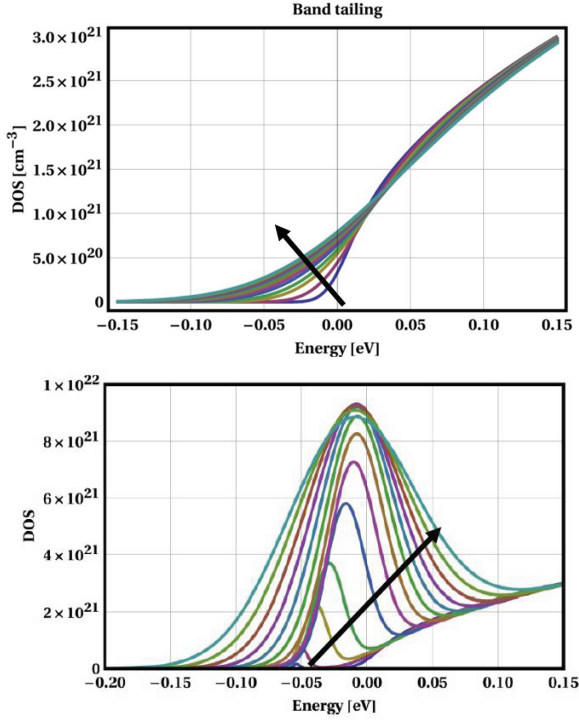


Fig. 4: The conduction band DOS (top) and the total DOS (bottom) for various doping conditions. From the bottom along the arrow, the donor concentration is, 10^{18} , 10^{19} , 5×10^{19} , and $i \times 10^{20}$ where $i = 1, 2, \dots, 10$

is the total screening length. The resulting conduction band DOS and the total DOS are plotted in Fig. 4. The acquired total DOS is used to calculate electron chemical potential and electron distribution. Applying charge neutrality equation, $n - p = N_D^+ - N_A^-$, is not helpful to calculate E_F because the impurity band is merged to the conduction band and the majority of the conduction electrons are from the impurity band at high doping condition. Therefore, we used the relation $N_D = n_{total}$ to find out the electron chemical potential, E_F . Here n_{total} includes all electrons occupying both the impurity band and the conduction band. Although overall band shape is metallic, we still discriminate the impurity band from the conduction band because the degeneracy factor is different.

$$N_D = \int_{-\infty}^{\infty} \left(\rho_i(E) \frac{1}{1 + 0.5 \exp\left(-\frac{E-E_F}{kT}\right)} + \rho_c(E) \frac{1}{1 + \exp\left(-\frac{E-E_F}{kT}\right)} \right) dE \quad (9)$$

Fig. 5 shows the E_F as a function of donor concentration at two temperatures (300K and 1000K). Interestingly, E_F monotonically increases beyond the original band edge as doping concentration increases. Previously it was believed that E_F is saturated near the E_C at high doping concentration because the added dopants create energy level below E_F . Monotonically increasing E_F explains why the Boltzmann statistics in diffusion model has been successful so far even at high doping condition. And Fig. 5 implies that existing theories assuming E_F saturation at the conduction band edge may need to be revised. Using the total DOS (Fig. 4) and E_F (Fig. 5), the actual electron distribution is plotted in Fig. 7 for three different total

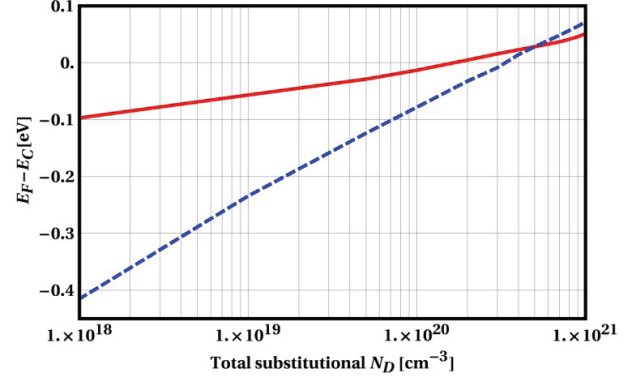


Fig. 5: E_F as a function of doping concentration at two different temperatures for As. (300K (red solid) and 1000K (blue broken))

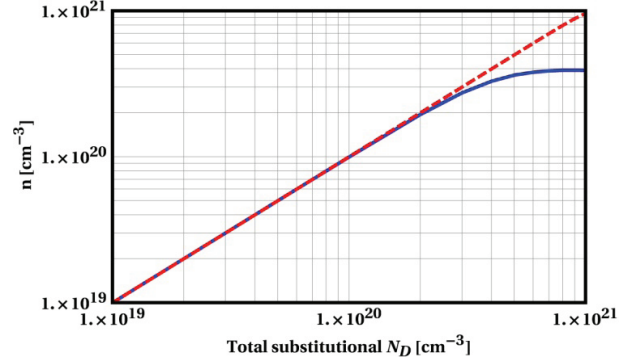


Fig. 6: Total electron concentration vs. active electron concentration at 300K (blue solid) and at 1000K (red broken)

concentrations. When electrons are distributed over a wide range of energy in a band, thermal excitation cannot promote electrons occupying deep levels to higher empty states and only electron within $\sim kT$ from E_F can contribute to the electric conduction. In our model, we choose the energy, $E_F - 2kT$, as the cut-off energy and electrons occupying the energy states below the cut-off energy are not counted as active. The chosen $2kT$ range gives a full activation up to $2 \times 10^{20} \text{ cm}^{-3}$ and saturation value about $4 \times 10^{20} \text{ cm}^{-3}$ at higher concentration. As shown in Fig. 6, while the active electron concentration is saturated at high doping concentration at 300K, all electrons are active at 1000K. It means that incorporating the impurity band model does not require modifying the existing diffusion model and thus adjusting the active concentration at the final stage of process simulation is justified.

IV. RESULT AND DISCUSSION

We applied donor pair model and impurity band model to diffusion simulation result and the results are plotted in Fig.8. The impurity band model alone greatly improves the previous result. The LMC model gives a retrograde active profile shape at extreme doping condition near the surface. The peculiar shape of LMC result cannot be confirmed with experimental data because the active profile near the surface is not provided in the original paper [2]. However, Giubertoni *et. al* showed a dramatic decrease in active dose after laser annealing when the peak concentration was around $5 \times 10^{21} \text{ cm}^{-3}$ [8], which is an indirect evidence of pairing effects. Considering the simplicity of the total vs. active electron relation (Fig.6), band only model can be

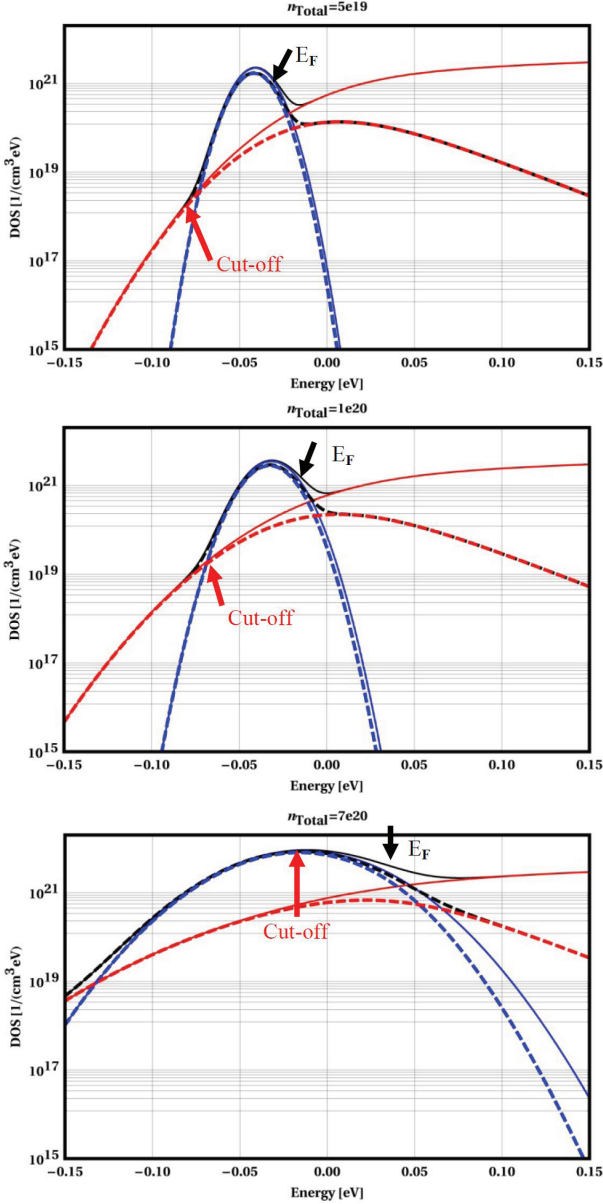


Fig. 7: Electron distribution in the band. Black solid lines are the total DOS which is overlapped by red solid line (the conduction band DOS) at the edges. Blue solid lines are the impurity band DOS. Broken lines are electron densities calculated by the product of DOS and Fermi distribution function for the obtained chemical potential, E_F . In each case, E_F and $E_{\text{cut-off}}$ are specified

a practical choice for conventional continuum simulation when doping concentration is below $5 \times 10^{21} \text{ cm}^{-3}$. When the total doping is beyond $5 \times 10^{21} \text{ cm}^{-3}$, LMC can make an important impact on the result. At this high doping, a large fraction of the dopants is within the 2NN spacing of other dopants. In this situation, the impurity band model alone cannot describe the system properly because it adds donor states as the Gaussian shape centered at $E_D + \Delta E_i$ although the dominant 1NN and 2NN DOS (Fig. 2) should add additional states to the lower energy side of the Gaussian center of the impurity band. In a point of view, LMC model combined with the impurity band model can be considered as an extended impurity band model because excluding closely spaced donor-donor pairs and donor-donorcluster pairs from the substitutional donor concentration is like adding impurity states to the low energy part of the impurity

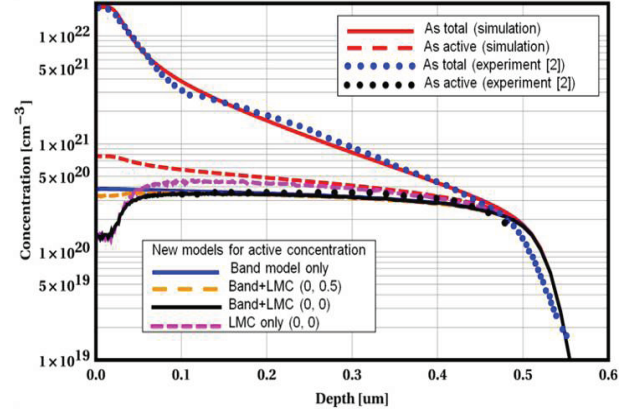


Fig. 8: As active concentration with new models. The number pairs for LMC represents the probability that As is inactive at the 1NN position of another As and $\text{As}_{\text{cluster}}$, respectively.

band. Therefore, introducing $\alpha(N_D)$ factor in Eq.2 to make the impurity band broaden quickly at very high doping condition is a flavor of the extended impurity band model. In a rigorous extended impurity band model, however, the factor should be a function of the total substitutional dopant concentration and cluster concentration: $\alpha(N_D, N_{Cl})$. More extensive statistical analysis and experimental data is required to develop the full impurity band model which is out of the scope of the study.

As the device design window becomes ever narrower, process simulation should be closely connected with device simulation. The presented model is an exemplary case connecting the missing part between process simulation and device simulation. The impurity band model can predict temperature dependent active electron concentration for the given total electron concentration which is beneficial to perform device simulation at various operation temperature conditions.

V. CONCLUSION

We have developed a donor deactivation model at high doping limit which includes the donor pair model and the impurity band model. The new models explain and reproduce the experimental results which cannot be done by existing models. By analyzing the band shape and chemical potential carefully, we have found that the activation limit of dopant having high chemical solubility originates from the nature of the impurity band, which is important for common donors like As and P in Si. The new models can provide useful information for doping strategy and the impurity band model itself also has a great importance in many other applications like device simulation and mobility model.

REFERENCES

- [1] Sentaurus Process, Synopsys Inc. <http://synopsys.com>
- [2] S. Solmi, and D. Nobili, J. Appl. Phys. **83**, 2484 (1998).
- [3] D.C. Müller, Ph.D. Thesis, Swiss federal institute of technology, Zurich (2004).
- [4] G. Kresse and J. Hafner, Phys. Rev. B **47**, RC558 (1993); G. Kresse and J. Furthmüller, **54**, 11169 (1996); VASP GUIDE, <http://www.vasp.at>.
- [5] N.F. Mott, Rev. Mod. Phys. **40**, 677 (1968).
- [6] T.F. Rosenbaum, R.F. Milligan, M.A. Paalanen, and R.N. Bhatt, Phys. Rev. B **27**, 7509 (1983).
- [7] T.F. Lee and T.C. McGill, J. Appl. Phys. **46** 373 (1975).
- [8] D. Giubertoni *et. al.*, J. Vac. Sci. Technol. B **28** C1B1 (2010).